

Novel expression of claudin-5 in glomerular podocytes

Ryo Koda · Linning Zhao · Eishin Yaoita · Yutaka Yoshida · Sachiko Tsukita ·
Atsushi Tamura · Masaaki Nameta · Ying Zhang · Hidehiko Fujinaka ·
Sameh Magdeldin · Bo Xu · Ichiei Narita · Tadashi Yamamoto

Received: 9 August 2010 / Accepted: 8 December 2010 / Published online: 27 January 2011
© Springer-Verlag 2011

Abstract Tight junctions are the main intercellular junctions of podocytes of the renal glomerulus under nephrotic conditions. Their requisite components, claudins, still remain to be identified. We have measured the mRNA levels of claudin subtypes by quantitative real-time PCR using isolated rat glomeruli. Claudin-5 was found to be expressed most abundantly in glomeruli. Mass spectrometric analysis of membrane preparation from isolated glomeruli also confirmed

only claudin-5 expression without any detection of other claudin subtypes. In situ hybridization and immunolocalization studies revealed that claudin-5 was localized mainly in glomeruli where podocytes were the only cells expressing claudin-5. Claudin-5 protein was observed on the entire surface of podocytes including apical and basal domains of the plasma membrane in the normal condition and was inclined to be concentrated on tight junctions in puromycin aminonucleoside nephrosis. Total protein levels of claudin-5 in isolated glomeruli were not significantly upregulated in the nephrosis. These findings suggest that claudin-5 is a main claudin expressed in podocytes and that the formation of tight junctions in the nephrosis may be due to local recruitment of claudin-5 rather than due to total upregulation of the claudin protein levels.

R. Koda and L. Zhao contributed equally to this work.

Electronic supplementary material The online version of this article (doi:10.1007/s00441-010-1117-y) contains supplementary material, which is available to authorized users.

R. Koda · L. Zhao · E. Yaoita (✉) · Y. Yoshida · Y. Zhang ·
S. Magdeldin · B. Xu · T. Yamamoto
Department of Structural Pathology, Institute of Nephrology,
Niigata University Graduate School of Medical
and Dental Sciences,
1-757 Asahimachi-dori,
Niigata 951-8510, Japan
e-mail: ren-path@med.niigata-u.ac.jp

R. Koda · I. Narita
Division of Clinical Nephrology and Rheumatology, Niigata
University Graduate School of Medical and Dental Sciences,
Niigata, Japan

S. Tsukita · A. Tamura
Laboratory of Biological Science, Graduate School of Frontier
Biosciences and Graduate School of Medicine, Osaka University,
Osaka, Japan

M. Nameta
Cooperative Laboratory of Electron Microscopy, Niigata
University,
Niigata, Japan

H. Fujinaka
Institute for Clinical Research, Niigata National Hospital,
Niigata, Japan

Keywords Glomerulus · Podocyte · Tight junction ·
Claudin-5 · Puromycin · Aminonucleoside

Introduction

Podocytes in the renal glomerulus are unique epithelial cells that allow the bulk flow of solute and water to pass through their paracellular space. It has been reported ultrastructurally that intercellular junctions of podocytes consist in slit diaphragms, tight junctions and gap junctions but not adherens junctions (Caulfield et al. 1976; Pricam et al. 1975; Rodewald and Karnovsky 1974). However, it remains controversial whether components of adherens junctions are contained in slit diaphragms (Reiser et al. 2000; Usui et al. 2003; Yaoita et al. 2002a). Slit diaphragms are unique to podocytes and predominant under physiological conditions. Tight junctions are occasionally found under physiological conditions but increase and become dominant

in nephrosis (Caulfield et al. 1976; Pricam et al. 1975; Ryan et al. 1975). The morphology of tight junctions is apparently different from that of slit diaphragms. Tight junctions form the closest contact between adjacent cells looking as if outer leaflets on the adjacent bilayers of cell membranes fused (Furuse and Tsukita 2006; Tsukita et al. 2008). In contrast, slit diaphragms bridge a very wide intercellular space, that is, the filtration slits between adjacent foot processes of podocytes and play critical roles in glomerular ultrafiltration (Rodewald and Karnovsky 1974). In spite of the morphological difference, the two intercellular junctions share some properties. Both of them function as paracellular permselective barriers. Tight junctions restrict paracellular ionic permeability. Slit diaphragms behave as a selective barrier restricting the passage of macromolecules through glomerular filtration slits. In addition, both junctions serve as a fence maintaining the polarized distribution of membrane proteins by restricting the intermixing of distinct apical and basolateral surface proteins. Slit diaphragm's fence-like function was shown by the distribution of podocalyxin, which is the major sialoprotein of the glomerulus (Schnabel et al. 1989). Some of components are shared by both junctions. ZO-1 and MAGI-1, proteins on the cytoplasmic face of tight junctions, are expressed on the cytoplasmic surface of foot processes at the point of insertion of slit diaphragms (Hirabayashi et al. 2005; Kurihara et al. 1992, Schnabel et al. 1990). It has been shown that podocytes under physiological conditions have abundant resources of tight junction components, because tight junctions are ubiquitously formed above slit diaphragms within a few minutes after rat kidneys are perfused with polycations such as protamine sulfate (Kerjaschki 1978; Kurihara et al. 1992; Seiler et al. 1977). The localization of the reserve components of tight junctions in normal podocytes remains obscure, although slit diaphragms are assumed to be one of the probable supply sources of the components (Zhao et al. 2008).

Claudins are tetraspan-transmembrane proteins, essential for barrier function and fence function of tight junction complex in epithelial and endothelial cells (Furuse and Tsukita 2006; Tsukita et al. 2008). At least 24 members of claudin have been reported in mice and humans with their tissue-specific distribution. Certain combinations of different claudin subtypes can assemble with each other on a plasma membrane of a single cell or between plasma membranes of apposing cells, so one could speculate that various subtypes and combinations of certain claudin subtypes might offer distinct functional property for tight junction complex and contribute to functional diversity of epithelial cells and endothelial cells in each organ.

To date, little is known which claudins podocytes express. We recently reported that claudin-6 was localized in tight junction of podocytes in the rat. However, other claudins might be constitutively expressed in podocytes,

because epithelial cells typically express multiple claudin subtypes and claudin-6 was not detected in human podocytes (Zhao et al. 2008). In the present study, we quantified mRNA levels of claudin subtypes in isolated glomeruli to narrow down possible candidates for claudin subtypes expressed in podocytes. Consequently, claudin-5 was found to be expressed most abundantly in glomeruli. Claudin-5 has been reported to be primarily present in tight junctions of endothelia (Morita et al. 1999) but in situ hybridization and immunohistochemistry showed that claudin-5 was localized exclusively in podocytes but not in glomerular endothelial cells.

Materials and methods

Animals

Wister-Kyoto rats were purchased from Charles River Japan (Atsugi, Japan) and were used in these experiments at the ages of 2 days and 8–10 weeks. Claudin-5-deficient mice were generated by mating heterozygous mutant mice as described previously (Nitta et al. 2003).

The procedures for the present study were approved by the Animal Committee at Niigata University School of Medicine and all animals were treated according to the guidelines for animal experimentation of Niigata University.

Antibodies

Following antibodies were used as primary antibodies: mouse monoclonal anti-claudin-5 antibody (clone: 4C3C2; Zymed laboratories, South San Francisco, CA, USA), rabbit anti-ZO-1 antibody (Zymed laboratories), goat anti-VE cadherin antibody (Santa Cruz biotechnology, Santa Cruz, CA, USA), rabbit anti-podocin antibody (kindly provided by Dr. H. Tsukaguchi, Kansai Medical University, Moriguchi, Japan) (Shono et al. 2007), rabbit anti-laminin antibody (DakoCytomation, Glostrup, Denmark), mouse monoclonal anti- β -actin (Sigma, St Louis, MO, USA).

Reverse transcription-PCR

Total RNA was extracted from isolated glomeruli, renal cortices, whole neonatal and adult kidney, lung and duodenum with TRIzol (Invitrogen, Carlsbad, CA, USA) according to the manufacturer's instruction. Glomeruli were isolated from cortices by a sieving method. Single-stranded cDNA was prepared from 5 μ g of RNA using SuperScript™ II Reverse Transcriptase (Invitrogen) and random hexamers (Takara Bio, Shiga, Japan). Thermal cycler Dice (Takara Bio) was used for amplification. The sequences of the primers are shown in Table 1. The PCR was performed

Table 1 Primers sets for PCR analysis

	Accession number	primers (forward, reverse)
Claudin-1	NM_031699	TTAGTGGCCACAGCATGGTA, GAAGGTGTTGGCTTGGGATA
Claudin-2	NM_001106846	GTGGCTGTAGTGGGTGGAGT, CCTGAGGTGAGCAGGAAAAG
Claudin-3	NM_031700	TATCCTACTGGCAGCCTTCG, GTTCCCATCTCTCGTTCTG
Claudin-4	NM_001012022	GATGGTCATCAGCATCATCG, GAAGCCACCAGAGGGTTGTA
Claudin-5	NM_031701	CACAGAGAGGGGTCGTTGAT, CTGCCCTTTCAGGTTAGCAG
Claudin-6	NM_001102364	CAGAGCCCTCTGTGCATCA, CCCTCCACCTATCAGCAAAA
Claudin-7	NM_031702	GGGGGAGATGACAAAGTGAA, CAGAAGGACCAGAGCAGACC
Claudin-8	NM_001037774	TATGACTCCCTGCTGGCTCT, CACCAGCGGGTTGTAGAAGT
Claudin-9	NM_001011889	AGAGGGTGTCTAGCTGGTTTG, TGCTTTTATTCCCAGGTTGG
Claudin-10	NM_001106058	CAGGTCTGTGTTCCATGACG, TTGATACTTGGTCCGGGAAG
Claudin-11	NM_053457	TGACCTGCAGCTACACCATC, GCCAGCAGAATAAGGAGCAC
Claudin-12	NM_001100813	CTGATTGGGATGTGCAACAC, GCTAGCGATCGTGACAAAACA
Claudin-13		
Claudin-14	NM_001013429	GCCCTACAGACCCTACCAG, TCCCCACGTTTACAAAAGGAC
Claudin-15	NM_001107135	TGGGAACGTCATCACCATA, CCCACCATGCCTAGAAAAGAG
Claudin-16	NM_131905	AGCGCTCCTCTCTCGTTTTA, TCCTAGGGGCCTTGTAGGAT
Claudin-17	NM_001107112	GACCGCCAATATCATCATCC, TGACCTTCTCTGGCTGTCT
Claudin-18	NM_001014096	GTCTGTGTTTGCCAACATGC, TTTGAAGTTGCGGTCATCAG
Claudin-19	NM_001008514	ACAGTAACCCCACTGCCAAG, GTGCAGCAGAGAAAGGAACC
Claudin-20	NM_001109394	TTTGCTGGAGGAGTCTGCTT, TCTCTGCTTGGGAGGGTAGA
Claudin-21		
Claudin-22	NM_001110143	CAGCATCTGGAGCTGAAACA, CTCACCTGGCCTCCGAATAG
Claudin-23	NM_001033062	CTGGGCTACCTAGGCAGTTG, ATGCTGACCCTCGCTGTAGT
Claudin-24		
GAPDH	XM_008463	TAAAGGGCATCCTGGGCTACACT, TTA CTCTTGGAGGCCATGTAGG

through 35 cycles of 94°C for 15 s, 62°C or 64°C for 30 s and 72°C for 1 min after pre-incubation at 94°C for 5 min using specific primers. After each PCR reaction, the accuracy of primers PCR products was confirmed by showing a single amplified product of the expected size in agarose electrophoresis and by sequencing after insertion of the PCR products into pGEM-T Easy vector (Promega, Madison, WI, USA) and cloning.

Quantitative real-time PCR analysis

Real time PCR analysis was performed using Light Cycler 1.5 PCR thermal cycler with FastStart DNA Master^{PLUS} SYBR Green I (Roche Diagnostics, Mannheim, Germany) as per the manufacturer's protocol. To quantify the amount of specific mRNA in the samples, a standard curve was generated for each run using pGEM-T Easy vector (Promega) containing the corresponding PCR products (dilution ranging from 1×10^1 copy/ μ l to 1×10^6 copy/ μ l). The ratio of claudin to glyceraldehydes-3-phosphate dehydrogenase (GAPDH) represents the consequence of ampli-

fication. The PCR was performed through 45 cycles of 95°C for 10 s, 62°C for 5 s and 72°C for 10 s. After each PCR reaction, the specificity of the PCR products was confirmed as a single peak in dissociation curve analysis.

Mass spectrometry

For identification of proteins in the membrane fraction of glomerulus, glomeruli isolated by a sieving method were homogenized in 3 volumes of 50 mM Tris-HCl, pH 7.5, 150 mM NaCl, 2 mM EDTA, 0.5 mM dithiothreitol and centrifuged at 600g for 10 min. The supernatant was centrifuged at 8,000g for 10 min and the resultant supernatant was further centrifuged at 105,000g for 60 min to obtain the membrane fraction as precipitate. The precipitate was subjected to solubilization in 0.5% TritonX-100, 0.25 M sucrose, 20 mM HEPES, pH 7.4, 1 mM dithiothreitol, 1 mM Na orthovanadate, 25 mM NaF, 0.5 mM PMSF, 4 μ g/ml pepstatin A, 4 μ g/ml leupeptin and solubilized proteins were recovered by centrifugation at 105,000g for 60 min. Western blotting analysis indicated

that most of the immunoreactivity to mouse anti-claudin 5 antibody was recovered in the supernatant. The solubilized proteins (25 μg) were separated on a 15% SDS-PAGE gel and silver-stained. The region of silver-stained gel in the molecular mass range from 20 to 30 kDa was manually cut into 4 equal slices (2 mm/slice), reduced with 10 mM dithiothreitol and carbamidomethylated with 55 mM iodoacetamide and subjected to in-gel trypsin digestion essentially as described previously (Katayama et al. 2001).

The tryptic digests were analyzed by two nanoflow HPLC-coupled with two different mass spectrometers; a linear iontrap-time-of-flight mass spectrometer (LIT-TOF MS, Hitachi NanoFrontier LD; Hitachi-High-Technologies, Tokyo, Japan) with a C18 separation column (0.050 \times 150 mm, MonoCap-FastFlow; GL Sciences, Tokyo, Japan) at a flow rate of 200 nl/min, or a iontrap mass spectrometer (IT-MS, 1100 LC/MSD XCT Trap; Agilent Technologies, Santa Clara, CA, USA) with a C18 separation column (Zorbax 300SB-C18, 3.5 μm , 0.075 \times 150 mm; Agilent Technologies) at a flow rate of 300 nl/min. In both approaches, mobile phases consisted in (A) 2% acetonitrile, 0.1% formic acid and (B) 98% acetonitrile, 0.1% formic acid. A linear gradient from 2 to 40% B for 100 min followed by 100% B for 20 min was applied to elute peptides when analyzed with LIT-TOF MS or a linear gradient from 2 to 40% B for 30 min followed by sequential isocratic runs with 50% B for 10 min and 80% B for 10 min when analyzed with IT-MS. The two most intense precursor ions were isolated in each mass survey scan and fragmented by collision-induced dissociation.

For raw data, files generated by the LIT-TOF MS were analyzed by data processing software (Hitachi-Hitechnologies) to create peak lists for acquired MS/MS spectra and used to search in the in-house built IPI_rat database (version 3.51) or Swiss-Prot database under taxonomy of rattus (version 56.3) by Mascot search engine (Matrix Science, version 2.21). Raw data files generated by the IT MS were analyzed by Spectrum Mill (Agilent Technologies; version 3.2.060) to create peak lists for MS/MS spectra and used to search in protein databases as described above by Spectrum Mill.

Search parameters for protein identification with Mascot were as follows: mass tolerance, ± 0.1 – 0.3 Da; fragment mass tolerance of ± 0.1 – 0.3 Da; missed cleavage, 2; fixed modification, carbamidomethylation on Cys; variable modifications, oxidation on Met and deamidation on Asn or Glu. For protein identification with Mascot only peptides exceeding the “identity” threshold were accepted as identified peptides by setting the significant threshold at 0.01–0.05 and expect cut-off to 0.01–0.05. False positive rates were estimated by searching against a randomized decoy database created by the Mascot Perl program. “Required bold red” was checked to allow identification of only the proteins with unique peptide matches.

Search parameters for protein identification with Spectrum Mill was the same with Mascot except that mass tolerance and fragment mass tolerance were set at ± 2.5 and ± 0.7 Da, respectively. For protein identification with Spectrum Mill, search results were autovalidated to select valid peptide matches on the basis of peptide scores and on the difference between scores against forward and reverse databases as well as rank 1 and rank 2 protein hits to exclude false positive peptide matches. Furthermore, the MS/MS spectra of autovalidated peptides were manually inspected to confirm that a series of at least three consecutive y- and b-ion fragments were ambiguously matched.

In situ hybridization

In situ hybridization was essentially carried out by using the Ribomap kit and Discovery automatic staining module (Ventana Medical Systems, Tucson, AZ, USA), essentially according to the manufacture’s instructions. Briefly, rat kidneys were fixed in 4% paraformaldehyde in PBS for 3 days at 4°C. Serial 6- μm kidney sections were automatically deparaffinized, fixed and acid treated. Then, the tissue sections were subjected to cell conditioning and protease digestion. Digoxigenin-labeled antisense and sense cRNA probes were synthesized by in vitro transcription using linearized templates (512 bp corresponding to bp 848–1,359 of rat *claudin-5* coding sequence, NM_031701). Hybridization was performed with antisense or sense probe (30 ng/side) at 60°C for 6 h in a Ribohybe hybridization solution (Ventana Medical Systems). Hybrids were detected with an alkaline phosphatase-conjugated antidigoxigenin antibody (Roche Diagnostics). Signal detection was performed with nitro blue tetrazolium chloride 5-bromo-4-chloro-3-indolyl phosphate 4-toluidinium salt as a chromogenic substrate at room temperature for 3 h in the dark.

Western blotting

Isolated glomeruli, renal cortices and medullae were homogenized in a lysis buffer containing 8 M urea, 1 mM dithiothreitol, 1 mM EDTA, 50 mM Tris-HCl pH 8.0 on ice. The homogenates were centrifuged at 20,000g to remove insoluble fractions. The protein concentration of samples was determined by Lowry’s method after precipitation by trichloroacetate with sodium deoxycholate (Peterson 1977). Then, 20 μg from protein of each sample was loaded on 15% sodium dodecyl sulfate-polyacrylamide gel and the bands were transferred to a polyvinylidene difluoride membrane. The membranes were preincubated with 5% non-fat milk in PBS containing 0.05% Tween 20, incubated with 0.5 $\mu\text{g}/\text{ml}$ of mouse monoclonal anti-claudin-5 antibody

or 1:10,000 diluted mouse monoclonal anti- β -actin antibody overnight and washed in PBS containing 0.05% Tween. They were incubated with a 1:500 diluted goat anti-mouse immunoglobulin conjugated with peroxidase-labeled dextran polymer (mouse EnVision; DAKO, Carpinteria, CA, USA) and the immunoreactivity was visualized using ECL plus a western blotting detection system (GE Healthcare, Buckinghamshire, UK). A densitometric analysis was performed using the NIH image software package (version 1.62, NIH).

Induction of experimental nephrosis

Puromycin aminonucleoside (PAN) nephrosis was induced in rats by intravenous injection of PAN (Sigma, Saint Louis, MO, USA) at a dose of 5 mg/100 g body weight in phosphate-buffered saline (PBS). Nephrotic rats were sacrificed at days 0, 2, 4, 6 and 10 after the PAN injection. Glomeruli were isolated and used as glomerular lysates for immunoblotting. For immunofluorescence microscopy, renal cortices were cut into small pieces and were snap-frozen with liquid nitrogen and stored at -80°C . For immunoelectron microscopy, kidneys were perfused with paraformaldehyde-lysine-periodate (PLP).

Immunofluorescence microscopy

The indirect immunofluorescence technique was applied to frozen kidney sections as described previously (Yaoita et al. 2002b). In brief, frozen kidneys were sectioned at a thickness of 3 μm in a cryostat, fixed in 2% paraformaldehyde for 10 min, washed with PBS 3 times, treated with 10% normal goat serum for 30 min and incubated with primary antibodies overnight. For double-label immunostaining, primary antibodies were premixed as follows and applied simultaneously: (1) mouse monoclonal anti-claudin-5 antibody (10 $\mu\text{g}/\text{ml}$) and rabbit anti-ZO-1 antibody (5 $\mu\text{g}/\text{ml}$) and (2) mouse monoclonal anti-claudin-5 monoclonal antibody (10 $\mu\text{g}/\text{ml}$) and goat anti-VE-cadherin antibody (4 $\mu\text{g}/\text{ml}$). After washing with PBS three times, the sections were incubated with TRITC-conjugated anti-rabbit IgG or anti-goat IgG for 1 h, washed with PBS again and incubated with FITC-conjugated anti-mouse IgG for 1 h. DAPI was used for nuclear staining. For double-labeling for claudin-5 and VE-cadherin, PBS or normal goat serum was used as a negative control. Immunofluorescence of the sections was observed with an Olympus microscope (BX50) equipped with epi-illumination optics and appropriate filters or with a laser scanning confocal microscope (A1Rsi; Nikon, Tokyo, Japan).

Immunoelectron microscopy

Immunoelectron microscopic observations of rat kidneys were carried out as reported previously (Zhao et al. 2008;

Yaoita et al. 2002b). In brief, 1-mm³ tissue blocks from PLP-perfused kidneys were placed in the PLP fixative for 4 h at 4°C , hydrated and then embedded in hydrophilic methacrylate resin. The ultrathin sections collected on nickel grids were stained with an immunogold technique. The sections were incubated with 5% normal goat serum for 1 h and then were incubated with mouse anti-claudin-5 antibody (5 $\mu\text{g}/\text{ml}$) for 1 h at room temperature, followed by 15 nm colloidal gold-AffiniPure goat anti-mouse IgG+IgM (H+L) (Seikagaku, Tokyo, Japan, 1:100 dilution) for 2 h. After washing in PBS and fixing with 2.5% glutaraldehyde, the sections were contrasted with uranyl acetate and lead citrate and were then viewed with a Hitachi H-600A electron microscope.

Statistics

Data were presented as the means \pm SD. A statistical assessment of the significance between control rats and PAN-treated ones was made using Student's *t* test. Differences were considered to be statistically significant at $p < 0.05$.

Results

Claudins expressed in rat isolated glomeruli

At least 24 members of claudin subtype have been reported in mice and humans (Angelow et al. 2008; Furuse and Tsukita 2006; Krause et al. 2008). We searched the database for the sequence of each rat claudin subtype and prepared primers except claudin-13, -21 and -24 of whose sequences were not found in the rat database. The primers used in this study are shown in Table 1. By using cDNA from a neonatal or adult whole kidney, lung or duodenum that have been reported to express some of the claudins (Krause et al. 2008), it was confirmed that each of the primers amplified gene fragments of the expected size by PCR. Among the claudins, claudin-1, -2, -4, -5, -6, -8, -10, -12, -15, -19 and -22 were detected in glomerular cDNA as a single band of PCR products in agarose electrophoresis. Because samples of isolated glomeruli contain tubular fragments and Bowman's capsule as minor components (Yaoita et al. 1991), absolute quantification of the amount of these claudin mRNAs was done by quantitative real-time PCR to narrow down the candidate claudins expressed in glomeruli. The expression levels of the claudins were standardized against GAPDH expression and compared. Consequently, claudin-5 was found to be expressed most abundantly in glomeruli (Fig. 1). The abundant expression of claudin-5 in glomeruli was corroborated by quantitative

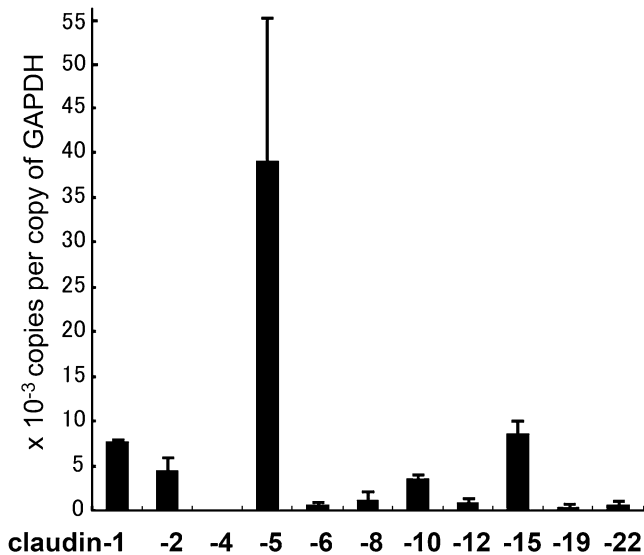


Fig. 1 Claudin mRNA levels detected in rat isolated glomeruli. Quantitative real-time PCR was performed with vectors containing each PCR product as a standard. Results are shown as the ratio of claudin to GAPDH and expressed as the mean \pm SD ($n=4$)

real-time PCR using different primer sets (Supplement Fig. S1).

Mass spectrometry was performed to identify claudins in membrane preparation of isolated glomeruli. By both approaches employing LIT-TOF MS and IT MS, only claudin-5 was identified. Although claudin-5 was identified with only one peptide match with sequence (EFYDPTVPVSQK) unique to claudin-5 in either analysis, the score exceeded the “identity” threshold in the Mascot search with a false positive rate less than 1% and the same

peptide was also credibly matched to claudin-5 by the Spectrum Mill search. Furthermore, the same peptide along with another peptide was found to match to claudin-5 in mass spectrometric analysis of immunoprecipitate from glomerular lysate with mouse monoclonal anti-claudin-5 antibody (data not shown). Taken together, mass spectrometric analysis could only identify claudin-5 with high-confidence, suggesting its predominance in membranes in the glomerulus.

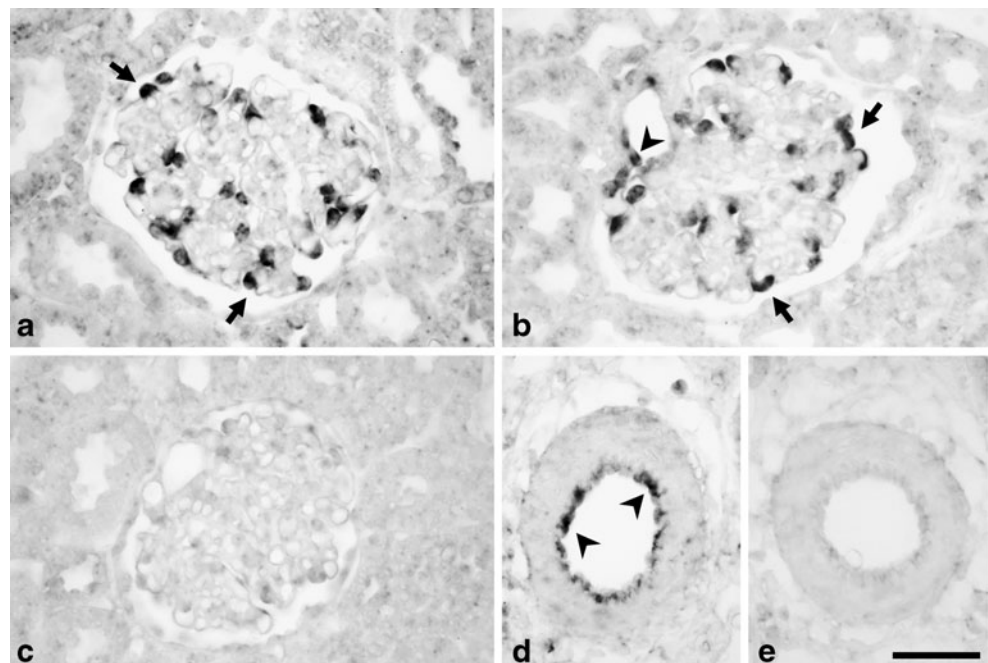
Claudin-5 mRNA localization in the glomerulus

To elucidate which cells in the glomerulus express claudin-5, the distribution of claudin-5 mRNA was assessed by in situ hybridization. Distinct signals for claudin-5 were found in cells on the surface of glomeruli, that is, podocytes (Fig. 2a–c). No significant signal was detected in capillary endothelial cells in glomeruli or the interstitium. Endothelial cells of arterioles were significantly stained at the vascular pole of glomeruli and in the interstitium (Fig. 2b, d).

Claudin-5 protein localization in podocytes

Claudin-5 distribution in the kidney was examined by western blot analysis and indirect immunofluorescence microscopy. Because rabbit antibody against carboxyl-terminal of claudin-5 did not react to any cells in the glomerulus as reported previously (Morita et al. 1999), we used a commercially available mouse monoclonal anti-claudin-5 antibody. Western blot analysis using neonatal kidneys from claudin-5-deficient mice was performed to examine the specificity of the antibody. Claudin-5-deficient mice were born in the expected Mendelian ratios and

Fig. 2 In situ hybridization using antisense (a, b, d) and sense (c, e) probes for claudin-5. a, b, c Distinct staining is found in cells facing the Bowman’s space, or podocytes (arrows) in the glomerulus, when hybridized with antisense probe (a, b) but not with sense probe (c). Capillary endothelial cells in the glomerulus and interstitium do not show significant staining but endothelial cells of arterioles at vascular pole (arrowheads) exhibit positive staining. d, e Endothelial cells (arrowheads) are stained significantly in the arterioles of the interstitium. Bar 50 μ m



looked normal macroscopically but all died within 10 h of birth (Niita et al. 2003). We examined the kidneys morphologically in claudin-5-deficient mice. No difference was found in their size, histology or ultrastructure between the deficient and wild mice (Supplement Fig. S2). Slit diaphragm proteins, ZO-1 and podocin, in the deficient mice were stained in the same way as wild mice (Supplement Fig. S3). The anti-claudin-5 antibody reacted with a distinct single band with a molecular mass of over 20 kDa in wild mice but not in claudin-5-deficient mice (Fig. 3a). Signals for claudin-5 were much more intense in the lysates from isolated glomeruli than those from cortices and medullae (Fig. 3b). In accordance with *in situ* hybridization, immunofluorescence microscopy showed that significant staining was found in glomeruli and arterioles (Fig. 4) but not in capillaries in the interstitium or epithelial cells of Bowman's capsule or tubular epithelial cells. No staining for claudin-5 was detected in the neonatal kidney of claudin-5-deficient mice (Fig. 5a), while distinct claudin-5 staining was observed in the wild mice (Fig. 5b). The above findings confirmed that the immunostaining was specific to claudin-5.

In the glomerulus, claudin-5 did not colocalize with VE-cadherin specifically expressed in endothelial cells (Lampugnani et al. 1995), indicating that glomerular endothelial cells were negative for claudin-5 (Fig. 5c). Double-labeled staining with anti-ZO-1 antibody showed distinct claudin-5 staining colocalized with ZO-1 along the glomerular capillary wall (Fig. 5d, d'). ZO-1 concentrates in slit diaphragms of podocytes (Schnabel et al. 1990). In addition, significant claudin-5 staining was observed in the outside of ZO-1 staining, or at the face of the urinary

space. The distribution suggested that claudin-5 may be localized not only at intercellular junctions of podocytes but also on apical cell membranes, that is, cell bodies and processes of podocytes. Actually, nuclei of podocytes were surrounded by claudin-5 staining (Fig. 5g). In the development, claudin-5 staining in podocytes became conspicuous at the S-shaped body stage (Fig. 5e). The staining was most intense at the apicalmost edges of the lateral cell membrane and less but significant along the basolateral cell membrane. Claudin-5 staining on the apical membrane was inconspicuous. At the capillary-loop stage, apical staining or cell body's staining was more conspicuous in addition to distinct staining along the capillary wall (Fig. 5f).

Claudin-5 protein localization in PAN nephrosis

Tight junctions in podocytes have been reported to increase in PAN nephrosis (Caulfield et al. 1976; Kurihara et al. 1992; Pricam et al. 1975; Ryan et al. 1975). Claudin-5 localization in the nephrotic condition was examined by indirect immunofluorescence microscopy. Measurement of 24-h urinary protein levels revealed that a single intravenous injection of PAN induced massive proteinuria at day 6 (116 ± 53 mg/day) and at day 10 (201 ± 39 mg/day). The staining on the apical surface of podocytes, easily detected in the normal condition, was reduced in the nephrotic condition (Fig. 5g, h). In addition, claudin-5 staining on the basal side of podocytes was almost continuous in the normal glomerulus but often discontinuous in the nephrotic condition (Fig. 5g, h).

The precise localization of claudin-5 in the glomerular capillary wall was examined by immunoelectron microscop-

Fig. 3 Western blot analysis of claudin-5 and β -actin using lysates from whole neonatal kidneys of wild (*wild*) and claudin-5 deficient (*KO*) mice (a) and using lysates from isolated glomeruli (G), cortices (C) and medullae (M) of normal kidneys of rats and mice (b)

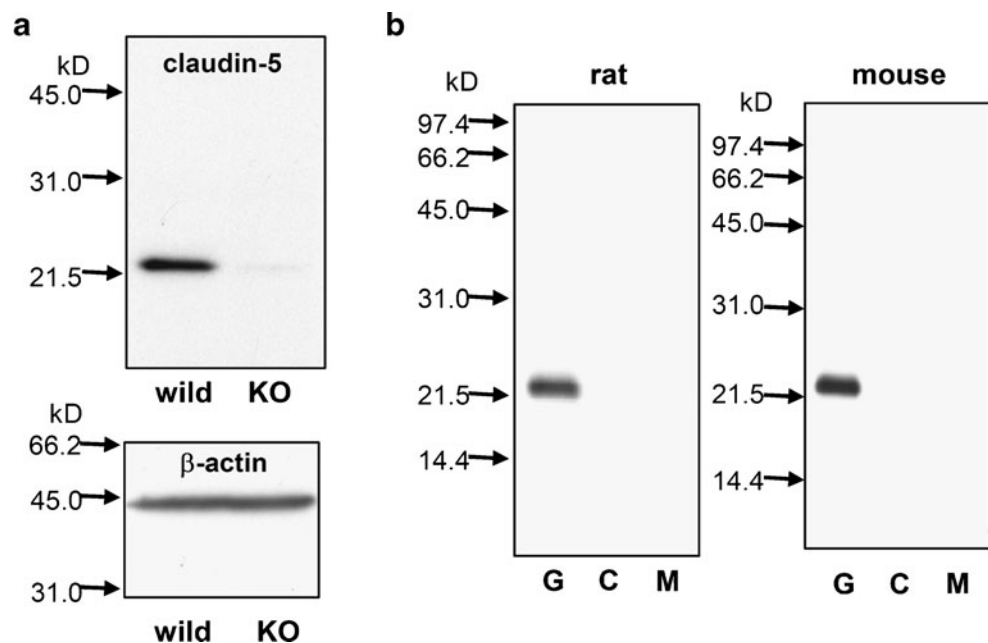
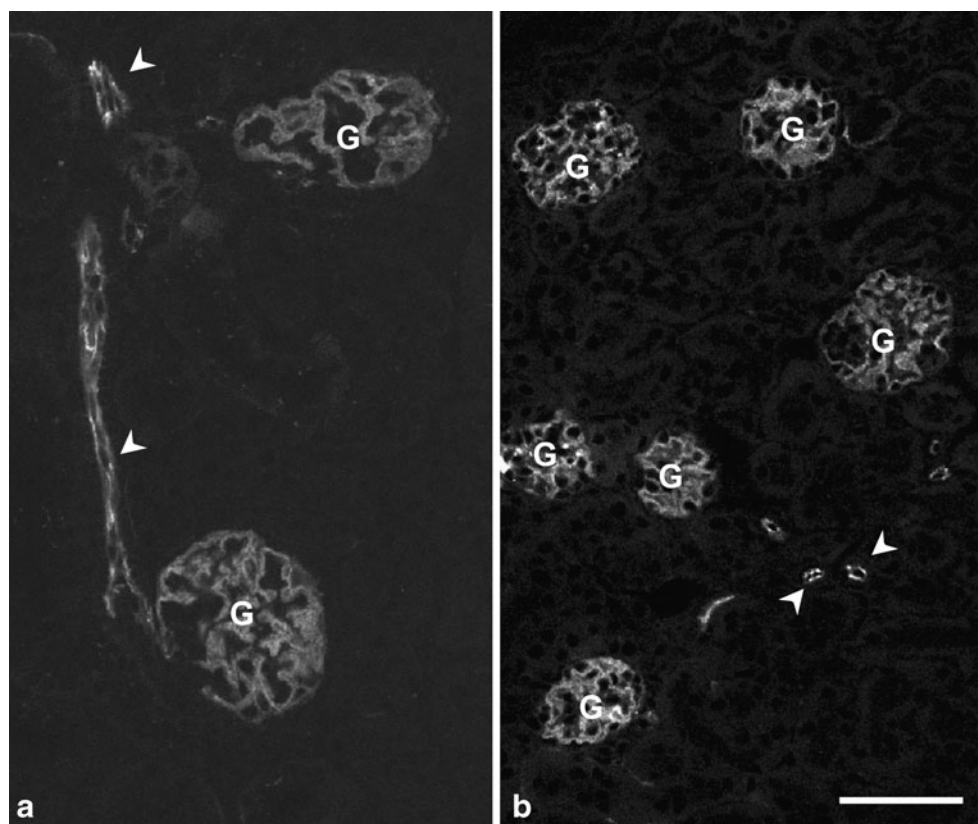


Fig. 4 Indirect immunofluorescence photomicrographs of frozen sections of rat (**a**) and mouse (**b**) kidneys incubated with antibodies against claudin-5. Glomeruli (*G*) and arterioles (*arrowheads*) exhibit significant staining. Bar 50 μm



py. In the normal kidney, immunogold particles for claudin-5 were found in most parts of podocytes, that is, on the apical and basal cell membranes, at the base of slit diaphragms and in the cytoplasm (Fig. 6a). Such immunogold particles were not observed in the negative controls using PBS instead of anti-claudin-5 antibody. In contrast, the immunogold particles were concentrated at close cell–cell contact sites including tight junctions in PAN nephrosis (Fig. 6b). During PAN nephrosis, the distribution of immunogold particles was significantly dislocated from the apical cell membrane and cytoplasm to newly formed cell–cell contact sites (Fig. 7). In endothelial cells of arterioles, claudin-5 particles were predominantly located at cell–cell contact sites (Figs. 6c and 7).

Western blot analysis was performed to quantify claudin-5 protein using isolated glomeruli from the different stages of PAN nephrosis (Fig. 8). Densitometric analyses of glomeruli did not show a significant difference between normal rats and rats 10 days after PAN injection.

Discussion

The novel finding in this study is claudin-5 expression in the glomerulus, especially in podocytes. Absolute quantitative real-time PCR analysis using isolated glomeruli showed that expression level of claudin-5 was the highest

in claudin subtypes (Fig. 1). Mass spectrometric analysis of membrane fractions from isolated glomeruli also confirmed claudin-5 expression without any detection of other claudin

Fig. 5 Indirect immunofluorescence photomicrographs of frozen sections of mouse (**a, b**) and rat (**c–h**) kidneys incubated with antibodies against claudin-5 (*green*; **a–h**), ZO-1 (*red*; **a, b, d', e, f**) and VE-cadherin (*red*; **c**). Nuclei were stained with DAPI (*blue*; **g, h**). **a, b** Double-labeled immunofluorescence photomicrographs for claudin-5 (*green*) and ZO-1 (*red*) in claudin-5-deficient (**a**) and wild (**b**) mouse kidneys. ZO-1 staining clarifies glomerular capillary wall (*G*) and tight junctions of endothelial cells in arterioles (*arrowheads*). Claudin-5 is not detected in the deficient mouse (**a**) but stained in the wild (**b**). Bar 50 μm . **c** Double-labeled immunofluorescence photomicrographs for claudin-5 (*green*) and VE-cadherin (*red*) in rat adult kidneys. Claudin-5 colocalizes with VE-cadherin only in arterioles (*arrowhead*) but not in glomerular or interstitial capillaries. Bar 50 μm . **d, d'** Double-labeled immunofluorescence photomicrographs for claudin-5 (*green*) and ZO-1 (*red*). Claudin-5 is detected outside ZO-1 staining (*arrowheads*) in addition to colocalizing with ZO-1 staining along the glomerular capillary wall. Bar 20 μm . **e, f** Double-labeled immunofluorescence photomicrographs for claudin-5 (*green*) and ZO-1 (*red*) in rat neonatal kidneys. Claudin-5 is seen at the apicalmost edges of the lateral membrane colocalizing with ZO-1 (*yellow*) and along the basolateral membrane in presumptive podocytes at the S-shaped body stage (**e**). The entire surface of podocytes including apical (*arrowheads*) and basolateral cell membrane is stained at the capillary-loop stage (**f**). Bar 25 μm . **g, h** Laser scanning confocal photomicrographs for claudin-5 in the glomerular capillary wall of normal (**g**) and nephrotic (**h**) kidneys. Apical staining of claudin-5 (*arrowheads*) is observed in the normal podocytes but not in the PAN nephrosis at day 10. Basal staining of podocytes was often discontinuous (*arrows*). Bar 10 μm . *Glomerular capillary lumen

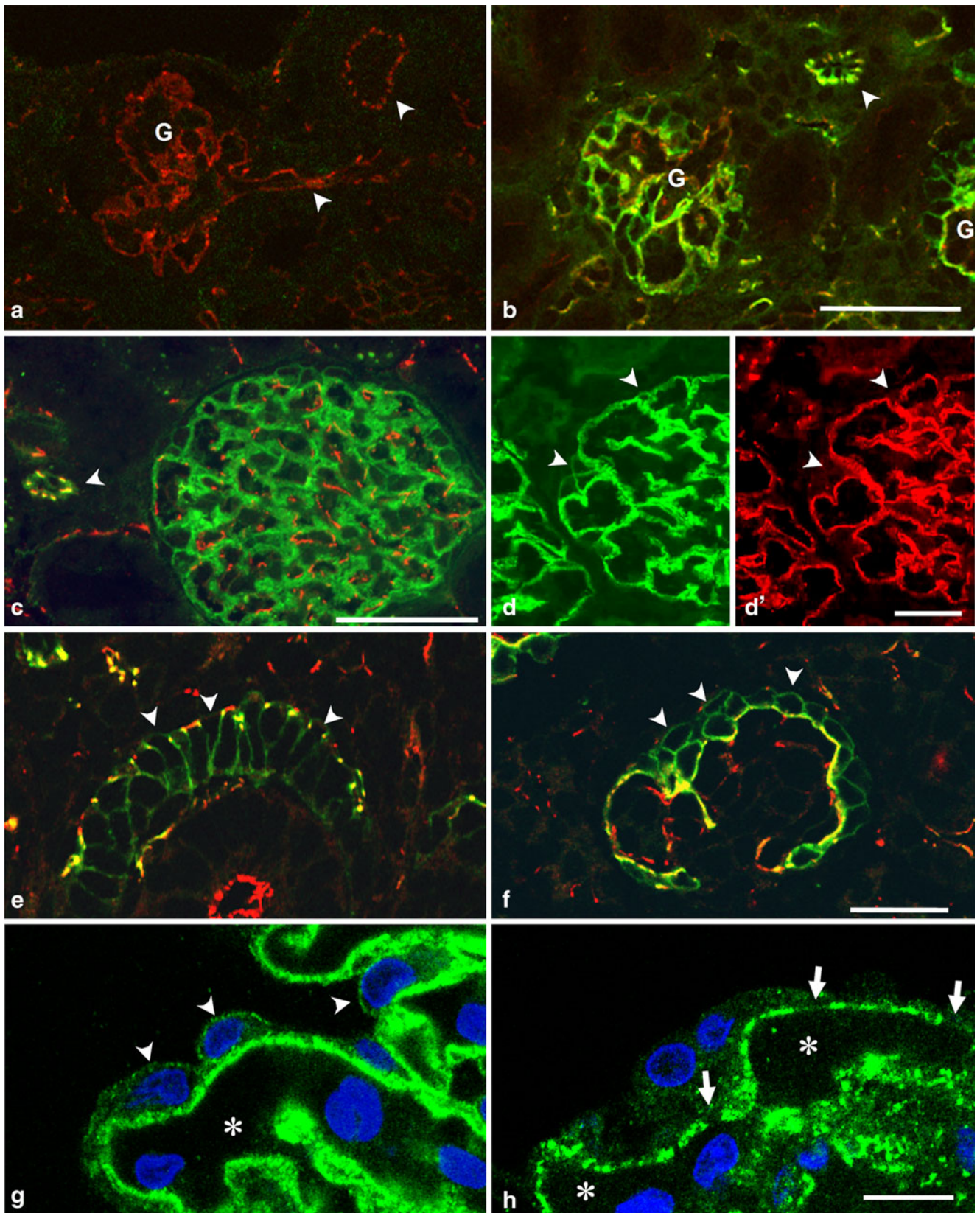
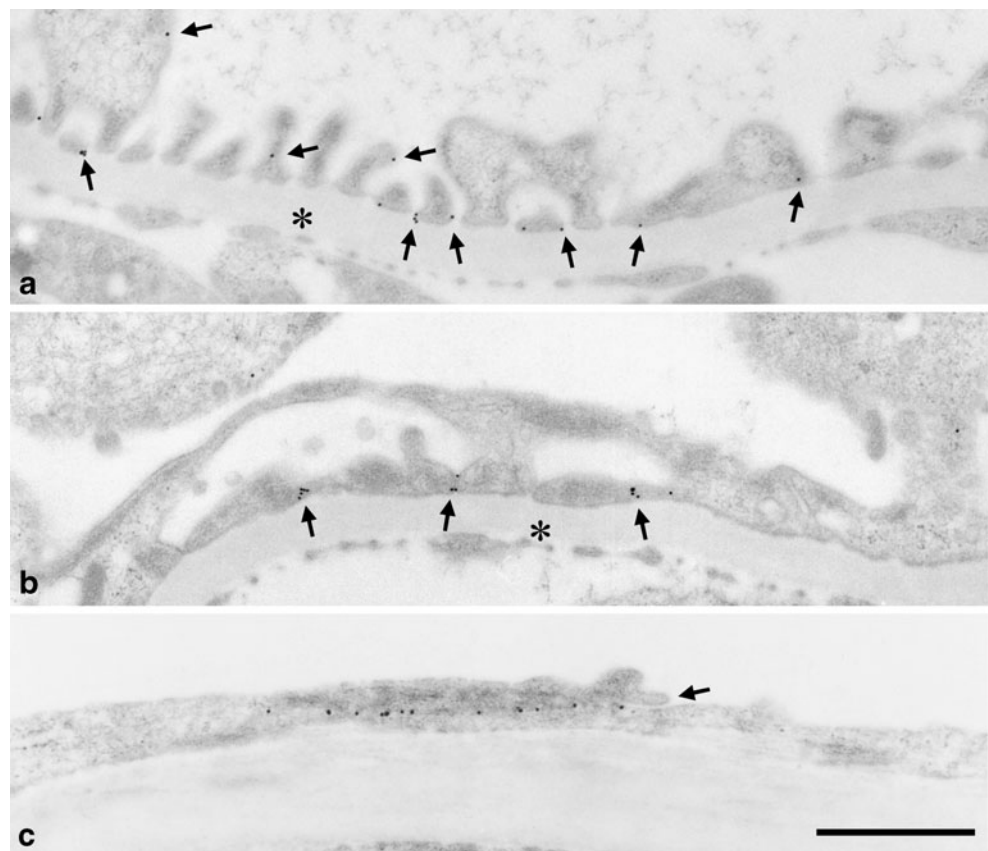


Fig. 6 Immunogold localization of claudin-5 in the glomerular capillary wall in normal (a) and PAN nephrotic (b) kidneys and endothelial cells of arterioles (c). Immunogold particles for claudin-5 (arrows) have a wide distribution in normal podocytes (a) but are located at cell–cell contact sites in podocytes of the nephrosis and endothelial cells of the arteriole (c). Bar 1 μm . *Glomerular basement membrane



subtypes. So far, claudin-3 and claudin-6 were reported to be expressed in mouse and rat podocytes, respectively. (Doné et al. 2008; Zhao et al. 2008). In PCR analysis in this study, claudin-3 was not amplified by PCR using rat isolated glomeruli. Claudin-6 was amplified but its expression level was much lower than claudin-5. These findings indicate that claudin-5 is the most abundant claudin expressed in the glomerulus. Western blot analysis showed that claudin-5 was dominantly localized in the glomerulus in the kidney (Fig. 3). In situ hybridization and immunofluorescence microscopy revealed that claudin-5 was expressed exclusively by podocytes in the glomerulus (Figs. 2, 4, and 5). It is proper to conclude that claudin-5 is the most abundant claudin expressed in podocytes and that podocytes are a unique epithelium expressing claudin-5 in the kidney.

Mouse monoclonal anti-claudin-5 antibody was obtained commercially and used in this study. Some commercially available antibodies against claudins, however, have been revealed to act as pan-claudin antibodies (Tsukita et al. 2008). Actually, preliminary experiments revealed that the monoclonal antibody stained all of COS7 transfectants expressing claudin-1, -3, -5 and -15. The staining was weak in claudin-1 and claudin-3 transfectants and the most intense in claudin-5 transfectants (data not shown). Western

blot analysis using the lysates from neonatal kidneys of claudin-5 deficient mice revealed weak but significant signals with the same size of claudin when X-ray films were exposed for longer times (data not shown). Thus, the antibody's crossreactivity with other claudins could not be excluded. Nevertheless, we concluded that the immunostaining using the antibody was specific to claudin-5 under the staining condition employed in this study, because no significant staining was observed in neonatal kidneys of claudin-5-deficient mice. In addition, mass spectrometric analysis detected only claudin-5 in the immunoprecipitation using glomerular lysates with the monoclonal antibody (data not shown). Identical localization of the immunostaining and in situ hybridization for claudin-5 also corroborated the immunostaining specificity to claudin-5 in the kidney.

The previous study reported that claudin-5 was not detected in the glomerulus by immunostaining using rabbit antibody against a polypeptide corresponding to the carboxyl terminal cytoplasmic domain of claudin-5 (Morita et al. 1999). There are at least two possible reasons for the discrepancy between the rabbit and mouse monoclonal antibodies. First, claudin-5 expressed in podocytes may lack the cytoplasmic domain including the antigen determinant recognized by the rabbit antibody. Second, the

antigen determinant recognized by the rabbit antibody may be hidden by binding associated proteins. The former is unlikely because both the antibodies reacted with equal-sized bands in western blot analysis using lysates of isolated glomeruli (data not shown). In addition, there is no report of claudin-5 lacking carboxyl terminal domain. Although we have assumed the latter possibility, further investigations are necessary to identify associated proteins such as immunoprecipitation.

Claudin-5 was observed on the entire surface of podocytes including apical and basal cell membrane in the normal condition. In endothelial cells of arterioles, claudin-5 was predominant at intercellular junctions. Claudin-5 has

been reported to be expressed by several types of epithelial cell including rat pancreas and gut (Rahner et al. 2001), chick retinal pigment epithelium (Kojima et al. 2002), rat alveolar epithelial cells (Wang et al. 2003), human ovarian surface epithelium (Zhu et al. 2006) and mouse prostate gland (Sakai et al. 2007). In most of the epithelial cells, claudin-5 is localized at cell–cell contact sites, especially at tight junctions. Only in gastric glands was the staining found along the basolateral cell membrane (Rahner et al. 2001). Hence, significant staining on the apical cell membrane is unique to podocytes. In the development of podocyte, the apical staining became distinct at the capillary-loop stage. At the earlier stage, claudin-5 staining is also observed in the renal vesicle before starting podocyte differentiation and in presumptive podocytes of S-shaped body stage but the apical staining was not intense (Fig. 5e, f; Supplement Fig. S4). In the capillary-loop stage, tight junctions in immature podocytes disappear with the opening of the intercellular spaces and the appearance of slit diaphragms. The reverse process occurs in nephrosis where slit diaphragms are extensively dislocated or disappear and tight junctions are frequently formed (Caulfield et al. 1976; Pricam et al. 1975; Ryan et al. 1975). As shown in this study, claudin-5 staining on the apical membrane became inconspicuous in PAN nephrosis (Fig. 5h). Relative localization by immunoelectron microscopy demonstrated that immunogold particles for claudin-5 significantly decreased on the apical cell membrane of nephrotic podocytes compared with normal podocytes (Fig. 7). Protein levels of claudin-5 were not significantly upregulated during PAN nephrosis, suggesting that claudin-5 accumulation at cell–cell contact sites of nephrotic podocytes may be due to local recruitment and not due to upregulation of the protein level. Apical distribution of claudin-5 and tight junction formation seem to be alternatively selected by podocytes, although the mechanism for altered distribution of claudin-5 needs further investigation.

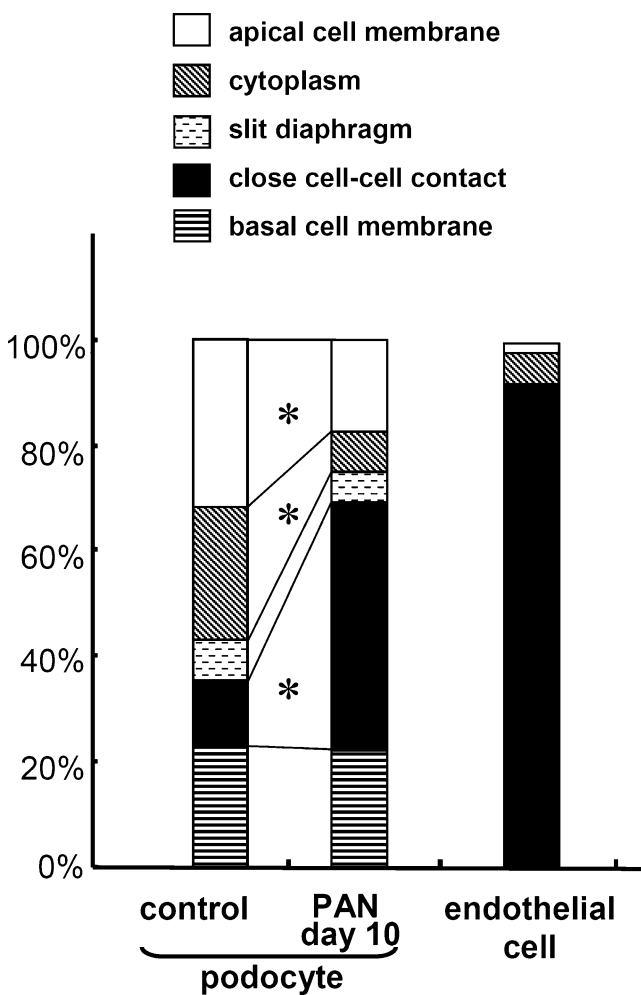


Fig. 7 Distribution of claudin-5 immunogold particles in rat podocytes and endothelial cells of arterioles. We examined the percentage distribution of the particles on the each part of the podocytes (i.e. apical cell membrane, cytoplasm, slit diaphragm, close cell–cell contact site, basal cell membrane,) in each glomerulus from different rats ($n=5$) and calculated means and standard deviation. $*p<0.05$ control rats versus PAN-treated rats

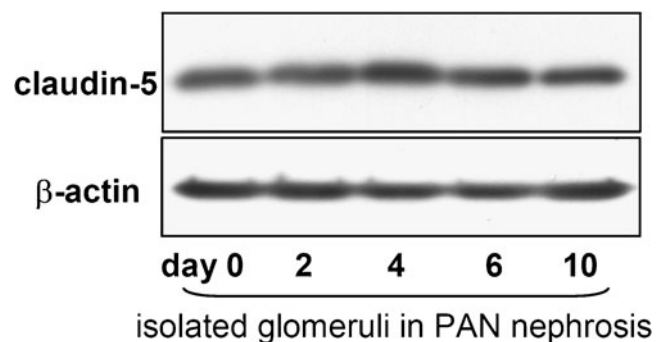


Fig. 8 Western blot analysis of claudin-5 and β -actin using lysates from isolated glomeruli in the time course of PAN nephrosis

Acknowledgments The authors thank Ms. Kanako Oda for her skillful assistance of transplantation of fertilized eggs and Dr. Kosei Takeuchi for helpful discussion and helping transfection of claudins to COS7 cells. This work was supported in part by a Grant-in-Aid for Scientific Research (C) from the Ministry of Education, Culture, Sports, Science and Technology (No. 21591021 to E.Y.).

References

- Angelow S, Ahlstrom R, Yu AS (2008) Biology of claudins. *Am J Physiol Renal Physiol* 295:F867–F876
- Caulfield JP, Reid JJ, Farquhar MG (1976) Alterations of the glomerular epithelium in acute aminonucleoside nephrosis. Evidence for formation of occluding junctions and epithelial cell detachment. *Lab Invest* 34:43–59
- Doné SC, Takemoto M, He L, Sun Y, Hultenby K, Betsholtz C, Tryggvason K (2008) Nephrin is involved in podocyte maturation but not survival during glomerular development. *Kidney Int* 73:697–704
- Furuse M, Tsukita S (2006) Claudins in occluding junctions of humans and flies. *Trends Cell Biol* 16:181–188
- Hirabayashi S, Mori H, Kansaku A, Kurihara H, Sakai T, Shimizu F, Kawachi H, Hata Y (2005) MAGI-1 is a component of the glomerular slit diaphragm that is tightly associated with nephrin. *Lab Invest* 85:1528–1543
- Katayama H, Nagasu T, Oda Y (2001) Improvement of in-gel digestion protocol for peptide mass fingerprinting by matrix-assisted laser desorption/ionization time-of-flight mass spectrometry. *Rapid Commun Mass Spectrom* 15:1416–1421
- Kerjaschki D (1978) Polycation-induced dislocation of slit diaphragms and formation of cell junctions in rat glomeruli: the effects of low temperature, divalent cations, colchicine, and cytochalasin B. *Lab Invest* 39:430–440
- Kojima S, Rahner C, Peng S, Rizzolo LJ (2002) Claudin 5 is transiently expressed during the development of the retinal pigment epithelium. *J Membr Biol* 186:81–88
- Krause G, Winkler L, Mueller SL, Haseloff RF, Piontek J, Blasig IE (2008) Structure and function of claudins. *Biochim Biophys Acta* 1778:631–645
- Kurihara H, Anderson JM, Kerjaschki D, Farquhar MG (1992) The altered glomerular filtration slits seen in puromycin aminonucleoside nephrosis and protamine sulfate-treated rats contain the tight junction protein ZO-1. *Am J Pathol* 141:805–816
- Lampugnani MG, Corada M, Caveda L, Breviario F, Ayalon O, Geiger B, Dejana E (1995) The molecular organization of endothelial cell to cell junctions: differential association of plakoglobin, β -catenin, and α -catenin with vascular endothelial cadherin (VE-cadherin). *J Cell Biol* 129:203–217
- Morita K, Sasaki H, Furuse M, Tsukita S (1999) Endothelial claudin: claudin-5/TMVCF constitutes tight junction strands in endothelial cells. *J Cell Biol* 147:185–194
- Nitta T, Hata M, Gotoh S, Seo Y, Sasaki H, Hashimoto N, Furuse M, Tsukita S (2003) Size-selective loosening of the blood-brain barrier in claudin-5-deficient mice. *J Cell Biol* 161:653–660
- Peterson GL (1977) A simplification of the protein assay method of Lowry et al. which is more generally applicable. *Anal Biochem* 83:346–356
- Pricam C, Humbert F, Perrelet A, Amherdt M, Orci L (1975) Intercellular junctions in podocytes of the nephrotic glomerulus as seen with freeze-fracture. *Lab Invest* 33:209–218
- Rahner C, Mitic LL, Anderson JM (2001) Heterogeneity in expression and subcellular localization of claudins 2, 3, 4, and 5 in the rat liver, pancreas, and gut. *Gastroenterology* 120:411–422
- Reiser J, Kriz W, Kretzler M, Mundel P (2000) The glomerular slit diaphragm is a modified adherens junction. *J Am Soc Nephrol* 11:1–8
- Rodewald R, Karnovsky MJ (1974) Porous substructure of the glomerular slit diaphragm in the rat and mouse. *J Cell Biol* 60:423–433
- Ryan GB, Leventhal M, Karnovsky MJ (1975) A freeze-fracture study of the junctions between glomerular epithelial cells in aminonucleoside nephrosis. *Lab Invest* 32:397–403
- Sakai N, Chiba H, Fujita H, Akashi Y, Osanai M, Kojima T, Sawada N (2007) Expression patterns of claudin family of tight-junction proteins in the mouse prostate. *Histochem Cell Biol* 127:457–462
- Schnabel E, Dekan G, Miettinen A, Farquhar MG (1989) Biogenesis of podocalyxin—the major glomerular sialoglycoprotein—in the newborn rat kidney. *Eur J Cell Biol* 48:313–326
- Schnabel E, Anderson JM, Farquhar MG (1990) The tight junction protein ZO-1 is concentrated along slit diaphragms of the glomerular epithelium. *J Cell Biol* 111:1255–1263
- Seiler MW, Rennke HG, Venkatachalam MA, Cotran RS (1977) Pathogenesis of polycation-induced alterations ("fusion") of glomerular epithelium. *Lab Invest* 36:48–61
- Shono A, Tsukaguchi H, Yaoita E, Nameta M, Kurihara H, Qin XS, Yamamoto T, Doi T (2007) Podocin participates in the assembly of tight junctions between foot processes in nephrotic podocytes. *J Am Soc Nephrol* 18:2525–2533
- Tsukita S, Yamazaki Y, Katsuno T, Tamura A, Tsukita S (2008) Tight junction-based epithelial microenvironment and cell proliferation. *Oncogene* 27:6930–6938
- Usui J, Kurihara H, Shu Y, Tomari S, Kanemoto K, Koyama A, Sakai T, Takahashi T, Nagata M (2003) Localization of intercellular adherens junction protein p120 catenin during podocyte differentiation. *Anat Embryol Berl* 206:175–184
- Wang F, Daugherty B, Keise LL, Wei Z, Foley JP, Savani RC, Koval M (2003) Heterogeneity of claudin expression by alveolar epithelial cells. *Am J Respir Cell Mol Biol* 29:62–70
- Yaoita E, Yamamoto T, Saito M, Kawasaki K, Kihara I (1991) Desmin-positive epithelial cells outgrowing from rat encapsulated glomeruli. *Eur J Cell Biol* 54:140–149
- Yaoita E, Sato N, Yoshida Y, Nameta M, Yamamoto T (2002a) Cadherin and catenin staining in podocytes in development and puromycin aminonucleoside nephrosis. *Nephrol Dial Transplant* 17(Suppl 9):16–19
- Yaoita E, Yao J, Yoshida Y, Morioka T, Nameta M, Takata T, Kamiie J, Fujinaka H, Oite T, Yamamoto T (2002b) Up-regulation of connexin43 in glomerular podocytes in response to injury. *Am J Pathol* 161:1597–1606
- Zhao L, Yaoita E, Nameta M, Zhang Y, Cuellar LM, Fujinaka H, Xu B, Yoshida Y, Hatakeyama K, Yamamoto T (2008) Claudin-6 localized in tight junctions of rat podocytes. *Am J Physiol Regul Integr Comp Physiol* 294:R1856–R1862
- Zhu Y, Brännström M, Janson PO, Sundfeldt K (2006) Differences in expression patterns of the tight junction proteins, claudin 1, 3, 4 and 5, in human ovarian surface epithelium as compared to epithelia in inclusion cysts and epithelial ovarian tumours. *Int J Cancer* 118:1884–1891